Journal of Innovative Optical Health Sciences
Vol. 6, No. 2 (2013) 1350011 (7 pages)

DOI: 10.1142/S1793545813500119

CHOP THERAPY INDUCED MITOCHONDRIAL REDOX STATE ALTERATION IN NON-HODGKIN'S LYMPHOMA XENOGRAFTS

H. N. XU[*,†], H. ZHAO[‡], T. A. MIR[*,†], S. C. LEE[*], M. FENG[*,†], R. CHOE[§], J. D. GLICKSON[‡] and L. Z. LI[*,†,¶,‖,**]

[*]*Department of Radiology*
University of Pennsylvania, Philadelphia, PA, USA

[†]*Britton Chance Laboratory of Redox Imaging*
Johnson Research Foundation
Department of Biochemistry and Biophysics
University of Pennsylvania, Philadelphia, PA, USA

[‡]*Biostatistics and Data Management Core*
The Children's Hospital of Philadelphia (CHOP), Philadelphia, PA, USA

[§]*Department of Biomedical Engineering*
University of Rochester, Rochester, NY, USA

[¶]*Abramson Cancer Center*
University of Pennsylvania, Philadelphia, PA, USA

[‖]*Institute of Translational Medicine and Therapeutics*
University of Pennsylvania, Philadelphia, PA, USA
[**]*linli@mail.med.upenn.edu*

Received 25 December 2012
Accepted 4 January 2013
Published 27 March 2013

Dedicated to the memory of late Dr. Britton Chance, who participated in the study with extraordinary scientific enthusiasm until the age of 97.

We are interested in investigating whether cancer therapy may alter the mitochondrial redox state in cancer cells to inhibit their growth and survival. The redox state can be imaged by the redox scanner that collects the fluorescence signals from both the oxidized-flavoproteins (Fp) and the reduced form of nicotinamide adenine dinucleotide (NADH) in snap-frozen tissues and has been previously employed to study tumor aggressiveness and treatment responses. Here, with the redox scanner we investigated the effects of chemotherapy on mouse xenografts of a human diffuse large B-cell lymphoma cell line (DLCL2). The mice were treated with CHOP therapy, i.e., cyclophosphamide (C) + hydroxydoxorubicin (H) + Oncovin (O) + prednisone (P) with CHO

administration on day 1 and prednisone administration on days 1−5. The Fp content of the treated group was significantly decreased ($p = 0.033$) on day 5, and the mitochondrial redox state of the treated group was slightly more reduced than that of the control group ($p = 0.048$). The decrease of the Fp heterogeneity (measured by the mean standard deviation) had a border-line statistical significance ($p = 0.071$). The result suggests that the mitochondrial metabolism of lymphoma cells was slightly suppressed and the lymphomas became less aggressive after the CHOP therapy.

Keywords: NADH; flavoprotein; DLCL2; therapeutic effect; tumor metabolism.

1. Introduction

Redox scanning is an *ex vivo* optical imaging method that can be applied to image the 3D tissue mitochondrial redox state with sub-millimeter high resolution based on the fluorescence signals of the endogenous NADH and Fp (including flavin adenine dinucleotide, i.e., FAD).[1,2] Mitochondrial NADH is the main source of the reducing equivalents for the mitochondrial respiratory chain. Mitochondrial metabolism is reflected in the redox state of the NAD system, which is tightly coupled with the flavin redox state in flavoproteins. The redox ratios, i.e., Fp/NADH, NADH/Fp, and Fp/(Fp+NADH), have been shown as sensitive biomarkers for the mitochondrial metabolic state.

Redox scanning has been used in cancer imaging to predict tumor aggressiveness and monitor treatment response. For example, the redox scanning indices have been shown to differentiate between an indolent and a metastatic breast cancer in mouse xenografts.[3] The tumor redox ratios correlated significantly with the invasive potentials of five melanoma lines xenografted in mice.[4] The redox scanning showed increased heterogeneity in the mitochondrial redox state in the pre-malignant mouse pancreases,[5] and also used to detect the metabolic changes in a glioma rat model under photodynamic therapy.[6] Additionally, the redox scanning has been employed to measure the cyclophosphamide-treatment effect on RIF-1 tumors in mice.[7] However, the redox scanning has not been applied to study the metabolic alterations in lymphomas subjected to CHOP treatment.

As the most common hematological cancer in the USA, lymphoma occurs in two forms, Hodgkin's Disease (HD) and Non-Hodgkin's lymphoma (NHL), the latter being the fifth most common cancer in the USA and far more common than HD. According to the American Cancer Society, in 2012, there were estimated ∼70,000 new NHL cases and ∼19,000 deaths from NHL in the USA.[8] The diffuse large B-cell lymphoma is the most common form of NHL and is characterized by the fast-growing tumors in the lymph nodes, spleen, liver, bone marrow, or other organs. The first-line standard therapy of NHL consists of 6−8 cycles of CHOP treatment,[9,10] where cyclophosphamide cross-links DNA; hydroxydoxorubicin (doxorubicin or adriamycin) intercalates between DNA bases and generates reactive oxygen species (ROS); oncovin (vincristine) binds to tubulin and inhibits cell duplication; and prednisone is a corticosteroid that suppresses inflammation. The effects of CHOP therapy on the mitochondrial redox state has not been reported previously.

Here, we present our initial redox scanning results on CHOP-treated DLCL2 xenografts in mice (models of the diffusive large B-cell lymphoma)[10] and demonstrate that the redox scanning has the potential to detect therapeutic effects on cellular metabolism in NHL. Some preliminary data have been reported in a conference proceeding.[30]

2. Materials and Methods

2.1. *Tumor xenografts and treatment*

WSU-DLCL2 cells were subcutaneously inoculated in the flanks of 5- to 7-week-old female nude mice to induce tumor xenografts.[11] Tumor-bearing mice were randomly chosen and divided into the treatment group and the control group. CHOP treatment is as follows: cyclophosphamide, 40 mg/kg i.v., day 1; hydroxydoxorubicin, 3.3 mg/kg i.v., day 1; oncovin, 0.5 mg/kg i.v., day 1; prednisone, 0.2 mg/kg p.o., days 1−5. Sham treatment was performed on the control group using saline. All animal studies were performed in accordance with the guidelines of the University of Pennsylvania Institutional Animal Care and Use Committee (IACUC).

2.2. *Redox scanning*

To harvest the lymphoma xenografts while maintaining their *in vivo* metabolic state, the anesthetized tumor-bearing mice were snap-frozen in liquid N_2 one day after the last treatment. The frozen tumors were quickly resected with a handsaw and then embedded in home-made mounting media followed by redox scanning as previously described.[3,12] Briefly, an excised frozen tumor was placed in the icy mounting media, then two frozen reference standards of FAD and NADH with known concentrations were carefully placed adjacent to the tumor. More icy mounting media slush was used to secure the tissue and the reference standards. Such embedded samples were milled to expose the tissue and the standards right before the redox scanning. The Fp channel excitation and emission filters were 430 ± 25 nm and 525 ± 32 nm, respectively; and those of the NADH channels were 360 ± 13 nm and 430 ± 25 nm, respectively. Each xenograft was scanned with three to five sections spacing $800-1000$ μm per tumor, with the first section approximately starting at about $1000-1500$ μm beneath the skin. Three tumors were scanned in each group.

2.3. *Data and statistical analysis*

The PC-collected scanning data were analyzed with a customized Matlab® program that uses the fluorescence intensity of the adjacently embedded reference standards to convert the intensity-based tissue images into the concentration-based images as detailed previously.[3,12] Briefly, the mean value of the fluorescence intensity of a specific reference standard was calculated and the background signal of the blank was subtracted, where the NADH standard served as the blank for the FAD standard and vice versa. The nominal NADH and Fp concentrations (in μM) in the tissue were calculated by comparing the tissue signal with that of the reference standards. The redox ratio Fp/(NADH + Fp) and NADH/Fp were generated on the basis of the nominal concentrations of Fp and NADH. A threshold of signal-to-noise ratio of 3 was used to exclude pixels with low signal intensity in either NADH or Fp channel. The values of these redox indices were first averaged for each tissue section to obtain the section mean values and standard deviations that will be used in the statistical analyses.

Since intratumor heterogeneity was easily seen from the redox images in both groups, the tissue spatial variations of the redox indices along the tissue depth (i.e., the distance from the immediate section beneath the skin to a specific section) should be taken into account for the statistical analysis. The Univariate analysis was conducted on these redox indices using IBM SPSS Statistics (version 20), where each of the redox indices was the dependent variable and treatment was the fixed factor (independent variable) with tissue depth as a covariate. The values of these indices were finally reported as mean ± SD along with the p-value showing the statistical significance.

3. Results

We measured the tumor volumes on day 1 and day 5. Table 1 shows the tumor volume ratios of day 5 to day 1. One cycle of CHOP administration reduced the volume of one tumor in the treated group, and the averaged tumor volume ratio of the treated group (1.20) was slightly less than those of the control group (1.34). However, we did not find significant changes in tumor volume between the two groups on either day 1 (Treated: $1001 \pm 50\,mm^3$ vs Control: $1204 \pm 728\,mm^3$) or day 5 (Treated: $1188 \pm 504\,mm^3$ vs Control: $1671 \pm 1025\,mm^3$); nor is the volume ratio of day 5 to day 1 significantly different between the two groups ($p > 0.05$).

Figures 1 (Treated) and 2 (Control) are the typical redox images. The quantitative results and the statistical analysis are summarized in Table 2. We see that the treatment has significantly decreased the Fp content from $565 \pm 227\,\mu M$ to $345 \pm 162\,\mu M$ ($p = 0.033$) and the Fp redox ratio from 0.53 ± 0.09 to 0.45 ± 0.07 ($p = 0.048$) as well as increased NADH/Fp from 1.01 ± 0.30 to 1.41 ± 0.39 ($p = 0.034$). No significant change was found in NADH. These results were further confirmed by the multivariate model (GLM, SPSS20),

Table 1. Tumor volume change.

Mouse #	*V_ratio (day5/day1)*	Mouse #	*V_ratio (day5/day1)*
Treated	—	Control	—
444	1.32	422	1.19
446	1.9	449	2.08
448	0.37	450	0.77

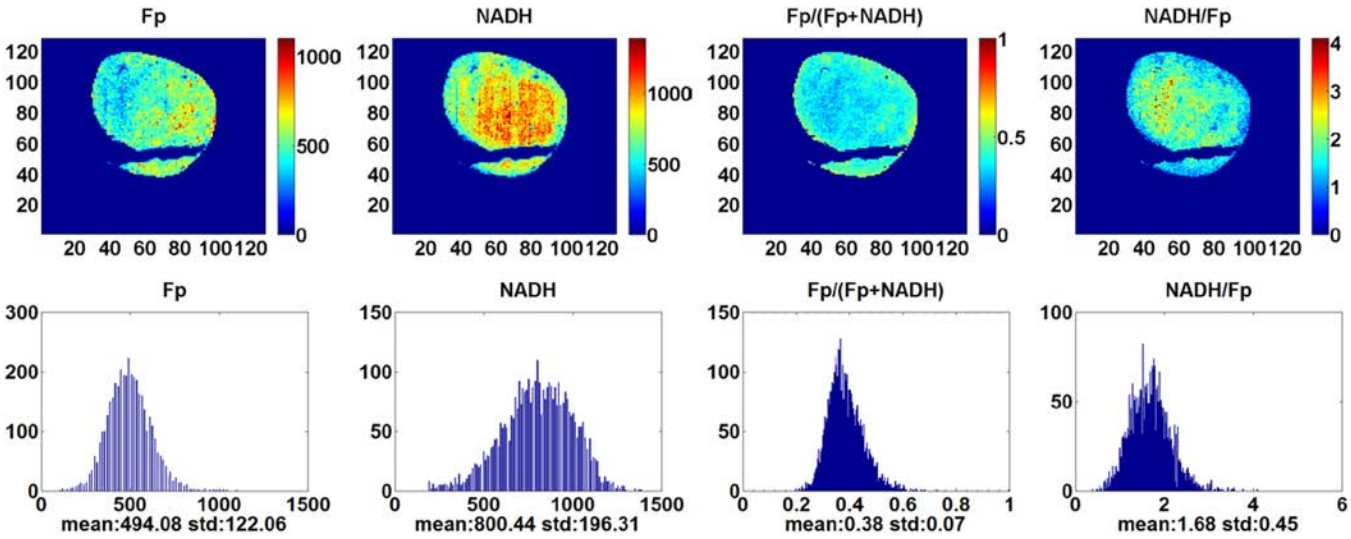

Fig. 1. Typical pseudo-color images of the redox indices (top row) and their corresponding histograms (bottom row) of a tumor in CHOP-treated group (1500 μm under the skin). From left to right: Fp nominal concentration (μM), NADH nominal concentration (μM), Fp redox ratio (0−1), and NADH/Fp. The mean value and SD are shown below the x-axes on each histogram. Image resolution: 200 μm.

Table 2. Mean values of the redox indices ± SD.

	Fp (μM)	NADH (μM)	Fp redox ratio	NADH/Fp
Ctrl (9 sections)	565 ± 227	450 ± 80	0.53 ± 0.09	1.01 ± 0.30
CHOP-Treated (11 sections)	345 ± 162	400 ± 172	0.45 ± 0.07	1.41 ± 0.39
P	0.033	0.54	0.048	0.034

where the four redox indices were the dependent variables, the treatment was the independent variable, and tissue depth was a covariate.

We also examined if the treatment had caused a significant change in the heterogeneity of the redox state. We used the mean standard deviation as a measure of tissue heterogeneity and a larger standard deviation indicates higher degree of tissue heterogeneity. As shown in Table 3, one-cycle of the treatment has caused tumors to become more homogeneous in Fp distribution with a borderline significance ($p = 0.071$). No significant change was found in the standard deviations of the other redox indices between the two groups ($p \geq 0.1$).

4. Discussions

Mitochondria may provide early biomarkers for cancer therapeutic response because of their central roles in cellular energy metabolism and apoptotic

Table 3. Mean values of the standard deviations of the redox indices ± SD.

	SD_Fp(μM)	SD_NADH(μM)	SD_Fp redox ratio	SD_NADH/Fp
Ctrl (9 sections)	256 ± 121	131 ± 25	0.11 ± 0.03	0.37 ± 0.12
CHOP-Treated (11 sections)	161 ± 99	117 ± 41	0.11 ± 0.03	0.52 ± 0.18
p	0.071	0.41	0.69	0.10

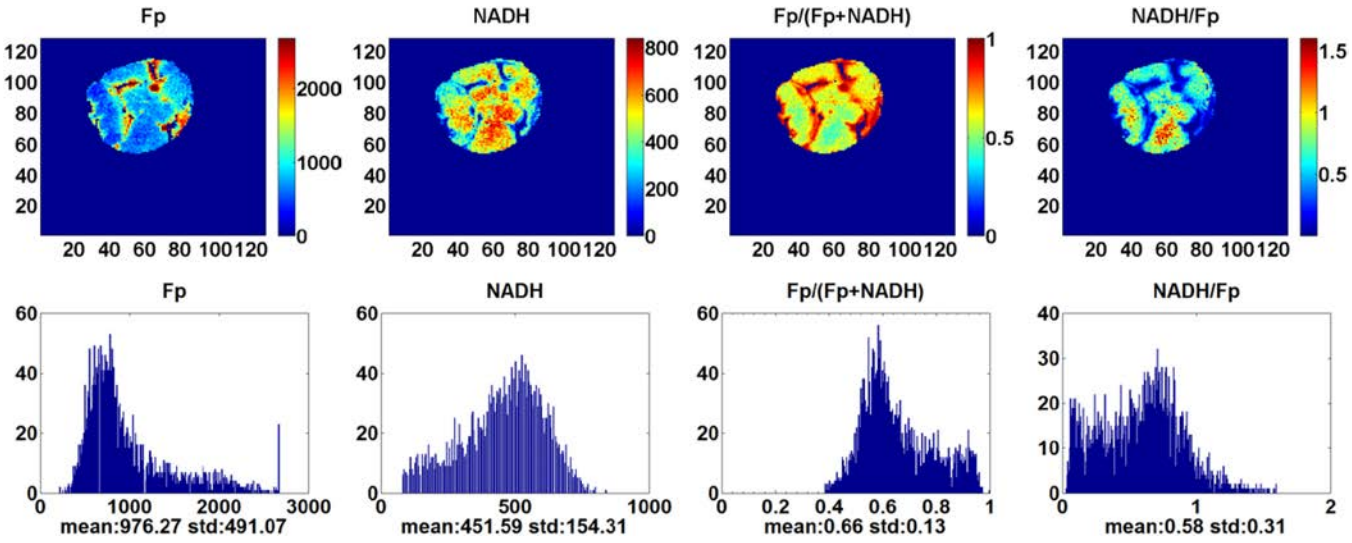

Fig. 2. Typical pseudo-color redox images (top row) and their corresponding histograms of a tumor in the control group (3500 μm under the skin). Image resolution: 200 μm.

signaling pathways that have been targeted by many cancer drugs.[13,14] A large body of studies have been performed *in vitro* on isolated mitochondria or cell culture to study the therapeutic effects of drugs on mitochondria. For instance, doxorubicin was shown to act on DNA independent of microtubules and did not induce the release of cytochrome c even at very high dosage using the isolated mitochondria from human cancer cells.[15] In cell cultures of some human cancer lines, the short-term (< 30 min) treatment with doxorubicin rendered the mitochondrial redox state of cancer cells more oxidized (more Fp and less NADH) with a large ROS production; whereas the long-term (48 h) treatment induced cell cycle arrest and cell death.[16] Vincristine is a cell-cycle−specific antitubulin agent that inhibits cell growth exclusively during metaphase by inhibiting microtubule dynamics and assembly leading to cell cycle arrest.[17−19] Investigations also showed that a substantial amount of tubulin inherently existed in the mitochondria and played a role in apoptosis through interaction with the permeability transition pore, whereas anti-tubulin agents could induce the release of cytochrome c from isolated mitochondria.[20] It was shown that the apoptotic cells have significantly higher Fp redox ratios.[21]

There are limited data showing how the tissue mitochondrial redox state is modified by therapy under *in vivo* condition. Redox scanning is the major method currently available to image tissue mitochondrial redox state *ex vivo* with a wide field of view (cm) and a submillimeter (50 μm) resolution.[22] A previous study[6] using redox scanning on a 9L glioma rat model showed that mitochondrial Fp redox state became more oxidized after photodynamic therapy. The observed higher Fp, lower NADH, and thus higher Fp redox ratio or more oxidized redox state were consistent with the oxidizing effects of the singlet oxygen generated in tissue by the photodynamic therapy. Redox scanning also indicated that cyclophosphamide treatment increased the NADH content along with decreased glycolytic rates and pO_2 in RIF-1 tumors in mice.[7]

In this study, we examined the therapeutic effect of CHOP on DLCL2 xenografts by *ex vivo* imaging the mitochondrial NADH and Fp fluorescent signals, and thus the mitochondrial redox state of the tumors across multiple tissue sections. Our results show that one 5-day cycle of CHOP treatment caused the decrease of Fp and shifted the lymphomas to a slightly more reduced mitochondrial redox state. As a calibration procedure is not available at the tissue level to determine the exact mitochondrial redox state as had been done *in vitro*,[23,24] we can only speculate that these lymphomas are likely to be mainly in either State 3 (active proliferation) or State 4 (at rest). State 2 (starvation) is unlikely due to relatively strong NADH signals, indicating the presence of sufficient reducing equivalents available for the mitochondrial electron transport chain. For States 3 and 4, higher Fp redox ratio

correlates with higher mitochondrial metabolism. Thus, the decrease of Fp redox ratio after treatment indicates suppressed mitochondrial metabolism. This is further supported by increased phosphomonoesters/βNTP ratio in our previous study[11] and decreased βNTP (nucleotide triphosphates) concentration (CHOP 2.0 ± 0.1 vs Sham $3.4 \pm 0.1\,\mu$mole/gram wet weight, unpublished data by SC Lee) after 3 cycles of CHOP treatment on DLCL2 xenografts as measured by ^{31}P-MRS on tissue extracts. That study also demonstrated a significant decrease in tumor lactate and proliferation rate, as measured by Ki67 staining after one cycle of CHOP therapy.[11] It appears that CHOP treatment may decrease both glycolysis and mitochondrial metabolism in DLCL2 xenografts. Although we are not certain about the exact mechanism, this result is consistent with a significant decrease of cell proliferation index Ki67 staining that was observable after 1 cycle of CHOP treatment.[11] As it was shown that cell density changes between the CHOP-treated and the control groups were insignificant,[11] the observed decreased Fp content and Fp redox ratio in CHOP-treated tumors in the present study should not be due to cell density differences. Our previous studies on melanoma and breast cancer mouse models indicated that the more metastatic tumors had more oxidized regions with higher Fp redox ratios, whereas the indolent tumors were relatively uniform and less oxidized.[3,4,22] Thus, the CHOP treatment appeared to induce a cellular metabolic change in the DLCL2 lymphomas toward less aggressiveness.

Since tissue heterogeneity has been regarded as one of the important characteristics of tumor malignancy,[25–29] we also investigated whether the CHOP treatment changed the heterogeneity of the redox state in tissue. The decrease of the Fp heterogeneity, although with a border-line significance ($p = 0.071$), appears to be consistent with the slight decrease of tumor aggressiveness.

It is well known that individuals often respond differently to the same cancer treatment. In the current study, one treated tumor had a large volume reduction and a higher Fp redox ratio compared to the other tumors. It is possible that one cycle of CHOP treatment had induced some apoptosis in this tumor. Co-registered histological investigations can be done in future studies to examine the correlation between the redox ratios and apoptosis in tumors.

5. Conclusions

To the best of our knowledge, this is the first study to explore the therapeutic effect of CHOP on the mitochondrial redox state of lymphomas. We presented the initial redox scanning data on the effects of CHOP treatment on DLCL2 xenografts and the corresponding statistical analyses. One-cycle of treatment caused the tumors to become slightly more reduced in their mitochondrial redox state, suggesting that the reduction in tumor metabolism and aggressiveness was induced by the treatment. We may conduct more in-depth studies with a larger sample size and more cycles of treatment in future.

Acknowledgments

The grant support to this work include the Center of Magnetic Resonance and Optical Imaging (CMROI) — an NIH-supported research resource P41RR02305 (R. Reddy), the Small Animal Imaging Resources Program (SAIR) 2U24-CA083105 (J. D. Glickson and L. Chodosh), 2R01-CA101700 (J. D. Glickson), and NIH K99/R00-CA126187 (R. Choe).

References

1. L. Z. Li, H. N. Xu, M. Ranji, S. Nioka, B. Chance, "Mitochondrial redox imaging for cancer diagnostic and therapeutic studies," *JIOHS* **2**, 325–341 (2009).
2. B. Quistorff, J. C. Haselgrove, B. Chance, "High spatial resolution readout of 3-D metabolic organ structure: An automated, low-temperature redox ratio-scanning instrument," *Anal. Biochem.* **148**, 389–400 (1985).
3. H. N. Xu, S. Nioka, J. D. Glickson, B. Chance, L. Z. Li, "Quantitative mitochondrial redox imaging of breast cancer metastatic potential," *J. Biomed. Opt.* **15**, 036010 (2010).
4. L. Z. Li, R. Zhou, H. N. Xu, L. Moon, T. Zhong, E. J. Kim, H. Qiao, R. Reddy, D. Leeper, B. Chance, J. D. Glickson, "Quantitative magnetic resonance and optical imaging biomarkers of melanoma metastatic potential," *Proc. Natl. Acad. Sci. USA* **106**, 6608–6613 (2009).
5. H. N. Xu, S. Nioka, B. Chance, L. Z. Li, "Heterogeneity of mitochondrial redox state in premalignant pancreas in a PTEN null transgenic mouse model," *Adv. Exp. Med. Biol.* **701**, 207–213, (2011).
6. Z. Zhang, D. Blessington, H. Li, T. M. Busch, J. Glickson, Q. Luo, B. Chance, G. Zheng, "Redox ratio of mitochondria as an indicator for the

response of photodynamic therapy," *J. Biomed. Opt.* **9**, 772−778 (2004).
7. H. Poptani, N. Bansal, W. T. Jenkins, D. Blessington, A. Mancuso, D. S. Nelson, M. Feldman, E. J. Delikatny, B. Chance, J. D. Glickson, "Cyclophosphamide treatment modifies tumor oxygenation and glycolytic rates of RIF-1 tumors: C-13 magnetic resonance spectroscopy, Eppendorf electrode, and redox scanning," *Cancer Res.* **63**, 8813−8820 (2003).
8. A. C. Society, Cancer Facts & Figures 2012, American Cancer Society, Atlanta (2012).
9. R. I. Fisher, E. R. Gaynor, S. Dahlberg, M. M. Oken, T. M. Grogan, E. M. Mize, J. H. Glick, C. A. Coltman, T. P. Miller, "Comparison of a standard regimen (CHOP) with three intensive chemotherapy regimens for advanced non-Hodgkin's lymphoma," *N. Engl. J. Med.* **328**, 1002−1006 (1993).
10. R. M. Mohammad, A. Al-Katib, A. Aboukameel, D. R. Doerge, F. Sarkar, O. Kucuk, "Genistein sensitizes diffuse large cell lymphoma to CHOP (cyclophosphamide, doxorubicin, vincristine, prednisone) chemotherapy," *Mol. Cancer Therap.* **2**, 1361−1368 (2003).
11. S.-C. Lee, M. Q. Huang, D. S. Nelson, S. Pickup, S. Wehrli, O. Adegbola, H. Poptani, E. J. Delikatny, J. D. Glickson, "In vivo MRS markers of response to CHOP chemotherapy in the WSU-DLCL2 human diffuse large B-cell lymphoma xenograft," *NMR Biomed.* **21**, 723 (2008).
12. H. N. Xu, B. Wu, S. Nioka, B. Chance, L. Z. Li, "Quantitative redox scanning of tissue samples using a calibration procedure," *JIOHS* **2**, 375−385 (2009).
13. S. Fulda, L. Galluzzi, G. Kroemer, "Targeting mitochondria for cancer therapy," *Nat. Rev. Drug Discov.* **9**, 447−464 (2010).
14. G. G. D'Souza, M. A. Wagle, V. Saxena, A. Shah, "Approaches for targeting mitochondria in cancer therapy," *Biochim. Biophys. Acta* **1807**, 689−696 (2011).
15. N. Andre, D. Braguer, G. Brasseur, A. Goncalves, D. Lemesle-Meunier, S. Guise, M. A. Jordan, C. Briand, "Paclitaxel induces release of cytochrome c from mitochondria isolated from human neuroblastoma cells," *Cancer Res.* **60**, 5349−5353 (2000).
16. A. V. Kuznetsov, R. Margreiter, A. Amberger, V. Saks, M. Grimm, "Changes in mitochondrial redox state, membrane potential and calcium precede mitochondrial dysfunction in doxorubicin-induced cell death," *Biochim. Biophys. Acta.* **1813**, 1144−1152 (2011).
17. S. Lobert, B. Vulevic, J. J. Correia, "Interaction of vinca alkaloids with tubulin: A comparison of vinblastine, vincristine, and vinorelbine," *Biochemistry* **35**, 6806−6814 (1996).
18. R. J. Owellen, C. A. Hartke, R. M. Dickerson, F. O. Hains, "Inhibition of tubulin-microtubule polymerization by drugs of the Vinca alkaloid class," *Cancer Res.* **36**, 1499−1502 (1976).
19. R. J. Owellen, A. H. Owens, Jr., D. W. Donigian, "The binding of vincristine, vinblastine and colchicine to tubulin," *Biochem. Biophys. Res. Commun.* **47**, 685−691 (1972).
20. M. Carre, N. Andre, G. Carles, H. Borghi, L. Brichese, C. Briand, D. Braguer, "Tubulin is an inherent component of mitochondrial membranes that interacts with the voltage-dependent anion channel," *J. Biol. Chem.* **277**, 33664−33669 (2002).
21. M. Ranji, D. L. Jaggard, B. Chance, "Observation of mitochondrial morphology and biochemistry changes undergoing apoptosis by angularly resolved light scattering and cryoimaging," *Proc. SPIE* 6087, 60870K (2006).
22. L. Z. Li, "Imaging mitochondrial redox potential and its possible link to tumor metastatic potential," *J. Bioenerg. Biomembr.* **44**, 645−653 (2012).
23. B. Chance, H. Baltscheffsky, "Respiratory enzymes in oxidative phosphorylation. VII. Binding of intramitochondrial reduced pyridine nucleotide," *J. Biol. Chem.* **233**, 736−739 (1958).
24. B. Chance, G. R. Williams, "A method for the localization of sites for oxidative phosphorylation," *Nature* **176**, 250−254 (1955).
25. I. J. Fidler, "Review: Biologic heterogeneity of cancer metastases," *Breast Cancer Res. Treat.* **9**, 17−26 (1987).
26. I. J. Fidler, I. R. Hart, "Biological diversity in metastatic neoplasms: Origins and implications," *Science* **217**, 998−1003 (1982).
27. G. H. Heppner, "Tumor heterogeneity," *Cancer Res.* **44**, 2259−2265 (1984).
28. G. H. Heppner, F. R. Miller, "The cellular basis of tumor progression," *Int. Rev. Cytol.* **177**, 1−56 (1998).
29. M. Gerlinger, A. J. Rowan, S. Horswell, J. Larkin, D. Endesfelder, E. Gronroos, P. Martinez, N. Matthews, A. Stewart, P. Tarpey, I. Varela, B. Phillimore, S. Begum, N. Q. McDonald, A. Butler, D. Jones, K. Raine, C. Latimer, C. R. Santos, M. Nohadani, A. C. Eklund, B. Spencer-Dene, G. Clark, L. Pickering, G. Stamp, M. Gore, Z. Szallasi, J. Downward, P. A. Futreal, C. Swanton, "Intratumor heterogeneity and branched evolution revealed by multiregion sequencing," *N. Engl. J. Med.* **366**, 883−92 (2012).
30. H. N. Xu, T. A. Mir, S. C. Lee, M. Feng, N. Farhad, R. Choe, J. D. Glickson, L. Z. Li, "Mapping the Redox State of CHOP-treated Non-Hodgkin's Lymphoma Xenografts in Mice," *Adv. Exp. Med. Biol.* (in press.)